CONDENSED
MATTER

Anomalous Josephson Effect in a Planar Hybrid Structure with the Spin−Orbit Coupling

A. V. Samokhvalov[a,b,*]

a Institute for Physics of Microstructures, Russian Academy of Sciences, Nizhny Novgorod, 603950 Russia
b Lobachevsky State University of Nizhny Novgorod, Nizhny Novgorod, 603950 Russia
***e-mail: samokh@ipmras.ru**

The way of formation of controlled phase inhomogeneity in a hybrid structure consisting of a short Josephson junction between two superconducting thin films, with one electrode partially coated with a ferromagnetic insulator, has been theoretically studied. The joint action of spin splitting and the Rashba spin−orbit coupling at the superconductor−ferromagnet interface leads to the generation of a spontaneous supercurrent, which changes the transport properties of the junction. The critical current and the current−phase relation of this hybrid structure have been calculated; it has been shown that this structure can be used to form an anomalous φ_0 Josephson junction with the phase shift φ_0 smoothly varying over a wide range.

Interest has recently increased in mesoscopic systems, which exhibit simultaneously superconductivity, spin−orbit coupling, and magnetism. Such superconducting structures with broken time reversal and spatial inversion symmetries [1] demonstrate two interesting interrelated phenomena: the anomalous Josephson effect (see [2] and references therein) and the superconducting (SC) diode effect [3]. The former effect concerns φ_0 Josephson junctions with an arbitrary phase difference φ_0 in the ground state, for which the current−phase relation can be written as $I(\varphi) = I_c \sin(\varphi + \varphi_0)$ [4, 5]. Here, φ is the phase difference between the superconducting electrodes and $|I_c|$ is the maximum (critical) supercurrent that may pass through the junction [6, 7]. In a particular case of $\varphi_0 = \pi$, a π junction is formed [8−11], which formally corresponds to the negative critical current $I_c < 0$ (see [12] and references therein). The anomalous Josephson effect can be implemented between superconductors with a unconventional type of pairing [13−15], in structures consisting of alternating 0 and π mini-junctions [4, 16−18], in junctions made of conventional singlet superconductors with a magnetic-metal barrier without inversion center [5, 19, 20], and in some other systems including quantum dots [21], semiconductor nanowires with the strong spin−orbit coupling [22], and topological insulators [23, 24]. Such φ_0 junction included in a closed contour induces an anomalous Josephson current and can be used as a phase battery [22, 25] or to control SC circuits and memory devices [26−28]. The superconducting diode effect implies nonreciprocal (more generally, anisotropic) transport, which is possible both in bulk materials [29−31] and in various SC systems [32, 33], including those based on Josephson junctions [34, 35].

The above-described ways of forming the φ_0 junction imply different mechanisms of creation of the phase difference due to specific features of tunneling through the barrier and/or the symmetry of the superconducting wavefunction. An alternative approach is to form a phase shift across the junction using an external magnetic flux penetrating the normal region [18, 36, 37] or current injection into the junction region on a scale smaller than the characteristic Josephson length [38−40]. Abrikosov vortices trapped in junction electrodes may be sources of high phase inhomogeneity near the junction [41−44]. The position of Abrikosov vortices in the junctions can be controlled by creating an additional pinning potential by means of microstructuring of SC electrodes [45] or by forming an array of submicron ferromagnetic particles near the superconductor surface [46−48] (their magnetization can be changed using a magnetic force microscope probe [49]). A change in the vortex position relative to the junction changes significantly the field dependence $I_c(H)$ [45], transport properties, and the current−phase relation of the Josephson junction and may be accompanied by the formation of the π state in this hybrid system [50].

In this work, we study the properties of the superconductor−ferromagnet hybrid structure serving as a tunable φ_0 junction, which consists of a planar Josephson junction with one SC electrode partially
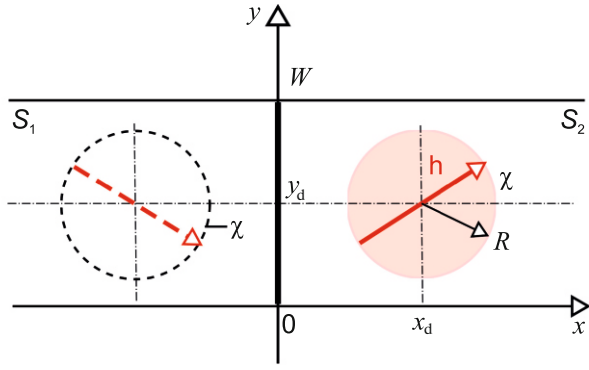
Fig. 1. (Color online) Schematic of the model superconductor–ferromagnetic structure: the planar Josephson junction in the plane $x = 0$ and the uniformly magnetized ferromagnetic insulator disk with the radius R centered at the point (x_d, y_d). The dashed line shows the "image" of the ferromagnetic insulator disk, the addition of which ensures both the absence of the normal x component of the supercurrent in the junction plane and the boundary condition given by Eq. (5).

coated with a ferromagnetic insulator (FI), the magnetic moment of which lies in the film plane (x, y) (Fig. 1). The exchange interaction between ferromagnetically ordered FI ions and conduction electrons of the metal induces the effective exchange field **h**, which significantly splits spin subbands [51–54] (see also [55, 56]). Because of the broken spatial inversion symmetry, the Rashba spin–orbit coupling $(\alpha_R/\hbar)[\mathbf{n} \times \mathbf{p}] \cdot \sigma$ is present in the surface layer with the thickness $l_{SO} \sim \hbar/\sqrt{2mE_g} \ll d$ near the superconductor–ferromagnet interface $(-l_{SO} \leq z \leq 0)$ [57, 58]. Here, **p** is the electron momentum, σ is the Pauli matrix vector, **n** is the unit vector directed along the normal to the superconductor–ferromagnet surface, E_g is the typical band gap in the FI, and $\alpha_R = \hbar v_R$ is the spin–orbit coupling constant, which is related to the Rashba velocity v_R [59]. The joint action of the exchange field, spin–orbit coupling, and superconducting pairing leads to the formation of a helicoidal state in the superconductor [60]; this state is characterized by the phase modulation of the superconducting order parameter ψ in the $[\mathbf{n} \times \mathbf{h}]$ direction and is current-free in spatially homogeneous systems [57, 58, 60, 61]. When the superconductor is coated partially with a ferromagnet, the helicoidal state is formed only in a limited region, which induces a supercurrent in the hybrid structure [62–65]. The resulting phase inhomogeneity, which serves as a phase battery [66, 67], and the related supercurrent make it possible to efficiently change the current–phase relation of the hybrid structure as a whole.

The model object under consideration is the superconductor–ferromagnet structure consisting of a Josephson junction between two s-type superconductor films S_1 and S_2 with the thickness d ($\lambda_F \ll d \ll \xi$)

and the width $W \ll \Lambda$, which are separated by a thin insulating layer (Fig. 1). An FI disk with the center at the point $\mathbf{r}_d = (x_d, y_d)$ and the radius $\xi \ll R \lesssim W/2$ is located on the surface of the planar junction electrode S_2. Here, ξ is the coherence length, λ_F is the Fermi wavelength of the superconducting metal in the normal state, and $\Lambda = \lambda^2/d$ is the Pearl screening length of the magnetic field in the film [68], which is related to the London depth $\lambda = (mc^2/4\pi c^2 n_s)^{1/2}$ for the bulk superconductor. At $d \ll \xi$, the exchange interaction in the SC film under the disk ($|\mathbf{r} - \mathbf{r}_d| \leq R$) can be considered as spatially homogeneous. On the assumption that the FI induces the exchange field h_{FI} in the surface layer with the thickness a, one can estimate the effective exchange-interaction energy $h \approx h_{FI}(a/d)$ [52–56]. Below, we consider only the case of sufficiently low temperatures and disregard the suppression of the superconducting order parameter $\psi = |\psi|e^{i\phi(\mathbf{r})}$ due to the inverse proximity effect at the superconductor–ferromagnet interface on the assumption that $|\psi|$ and Λ are identical throughout the SC film. It is also assumed that the distance from the junction to the disk is not too small ($x_d - R \gg \xi$) and there are no Pearl vortices [68], which can be formed near the FI disk edges [65, 69–71]. On these assumptions, the free-energy functional of the hybrid structure under consideration should be supplemented with a momentum-linear term (Lifshitz invariant), which can be written for the London model in the form [64]

$$\mathscr{F}_L = \frac{\alpha_R l_{SO}}{E_F}|\psi|^2 \int d\mathbf{r}[\mathbf{h}(\mathbf{r}) \times \mathbf{n}]\left(\nabla\phi + \frac{2\pi}{\Phi_0}\mathbf{A}\right). \quad (1)$$

Here, $\Phi_0 = \pi\hbar c/e$ is the magnetic flux quantum ($e > 0$), where $\hbar$ is the reduced Planck constant, c is the speed of light in vacuum, and e is the elementary charge; E_F is the Fermi energy in a superconducting metal; and $\mathbf{r} = (x, y)$ is the position vector in the structure plane. Note that the contribution from $\mathscr{F}_L$ to the free energy of a superconductor with the broken spatial inversion symmetry (along the direction **n**) and in the presence of the exchange or Zeeman field **h** can be justified on only symmetry considerations [72, 73].

The occurrence of the inhomogeneous helicoidal state in a limited region of the SC film under the FI disk leads to the generation of spontaneous supercurrent, the distribution of which in the London approximation including the gradient term (1) and the Josephson junction in the plane $x = 0$ is described by the expression

$$\mathbf{g}(\mathbf{r}) = -\frac{c\Phi_0}{8\pi^2\Lambda}\left(\nabla\phi + \frac{2\pi}{\Phi_0}\mathbf{A} - \upsilon + \alpha(\mathbf{r})\right), \quad (2)$$

where ∇ denotes the gradient in the (x, y) plane. The parameter

$$\alpha(\mathbf{r}) = \alpha_0[\mathbf{e}_h, \mathbf{z}_0], \quad \alpha_0 = \frac{4\pi l_{SO}}{d\lambda_R}\frac{h}{E_F}, \quad (3)$$

where $\mathbf{e}_h$ is the unit vector along the exchange field and $\lambda_R = 2\pi\hbar/(mv_R)$ is the wavelength corresponding to the Rashba momentum, is nonzero in the region covered with the FI disk and characterizes the joint action of the exchange field $\mathbf{h} = h\mathbf{e}_h$ and the Rashba spin–orbit coupling. The vortex source υ is determined by the gradient of the Josephson phase difference $\partial_y\varphi(y)$ across the junction [74]:

$$\nabla \times \upsilon = \partial_y\varphi\delta(x)\mathbf{z}_0, \quad \nabla \cdot \upsilon = 0. \quad (4)$$

For the simplest sinusoidal dependence of the Josephson current on the phase difference $j = j_c\sin\varphi$, the current component $\mathbf{g}$ normal to the junction should satisfy the following condition in the junction plane:

$$g_x(0,y) = g_c\sin(\varphi(y)), \quad g_c = j_cd.$$

In the planar junction with the critical current density j_c at $d \ll \lambda$, the parameter $L = \lambda_J^2/\lambda = c\Phi_0/16\pi^2\Lambda g_c$ acts as the Josephson length $\lambda_J = (c\Phi_0/16\pi^2\lambda j_c)^{1/2}$ [75], and the contribution from the vortex source υ (4) to the supercurrent $\mathbf{g}(\mathbf{r})$ (2) can be disregarded [76]. On the assumption that the critical current of the junction is low (in comparison with the currents induced in the film by the FI disk), the low electron transparency of the insulating barrier can be neglected, and it will be assumed below that $j_c = 0$. This simplest approximation corresponds to the zero boundary condition for the supercurrent component $g_x(\mathbf{r})$ in the junction electrode S_2,

$$g_x(0,y) = 0, \quad (5)$$

and allows for an analytical solution, which makes it possible to qualitatively describe the expected effect. In the case under consideration (a narrow SC strip interrupted by the Josephson junction), the screening effect and the influence of the magnetic field generated by this current can be neglected. The current distribution $\mathbf{g}(\mathbf{r})$ is determined mainly by the term $\nabla\phi$ ($\Phi_0|\nabla\phi|/|\mathbf{A}| \sim \Lambda/W \gg 1$), while the contribution from the vector potential $\mathbf{A}$ in Eq. (2) can be disregarded. The y component of the supercurrent $\mathbf{g}(\mathbf{r})$ (2) should be absent at the edges of the SC strip ($y = 0, W$), which corresponds to the boundary conditions

$$g_y(x,0) = g_y(x,W) = 0. \quad (6)$$

The condition $\text{div}\mathbf{g}(\mathbf{r}) = 0$, expression (2), and boundary conditions (5) and (6) make it possible to calculate the distributions of the SC order parameter and supercurrent generated in a narrow SC strip with

the planar Josephson junction under the exchange field of the FI disk and the Rashba spin–orbit coupling at the superconductor–ferromagnet interface.

The substitution of Eq. (2) into the condition $\text{div}\mathbf{g}(\mathbf{r}) = 0$ gives the two-dimensional Poisson's equation

$$\Delta\phi(\mathbf{r}) = -\text{div}\alpha(\mathbf{r}), \quad (7)$$

which, along with the boundary conditions (5) and (6), describes the distribution of the order parameter phase $\phi(\mathbf{r})$ in the junction electrode S_2 with the FI disk (i.e., at $x \geq 0$ in this case (see Fig. 1)). In the aforementioned approximations (where screening effects are neglected ($\mathbf{A} = 0$) and the Josephson current through the absolutely non-transparent barrier is absent ($j_c = 0$)), there is no supercurrent in the left electrode S_1, and the homogeneous state is established with the wavefunction whose phase can be assumed to be zero for certainty. Boundary condition (5) can be satisfied using the image method and by adding the supercurrent formed by the FI disk with the center at $(-x_d, y_d)$, radius R, and exchange field $\tilde{\mathbf{h}} = h(\mathbf{x}_0\cos\chi - \mathbf{y}_0\sin\chi)$. In view of the linearity of Eq. (7) and boundary conditions (5) and (6), the desired solution of Eq. (7) at $x \geq 0$ can be presented as

$$\phi(\mathbf{r}) = \phi_+^\alpha(\mathbf{r}) + \phi_-^\alpha(\mathbf{r}) + \psi(\mathbf{r}). \quad (8)$$

Here, $\phi_\pm^\alpha(\mathbf{r})$ is the solution of Poisson's equation (7) in an infinite film with the FI disk with the sources on the right-hand side that are nonzero in the regions $r_\pm^2 = (x \mp x_d)^2 + (y - y_d)^2 \leq R^2$ and are characterized by the exchange field $\mathbf{h} = h(\mathbf{x}_0\cos\chi \pm \mathbf{y}_0\sin\chi)$ (see the supplementary materials):

$$\phi_\pm^\alpha(\mathbf{r}) = \frac{\alpha_0}{2}\left[\mp(x \mp x_d)\sin\chi + (y - y_d)\cos\chi\right]$$
$$\times\begin{cases} 1, & r_\pm < R \\ (R/r_\pm)^2, & r_\pm > R \end{cases}. \quad (9)$$

The function $\psi(\mathbf{r})$ in Eq. (8) is the solution of the two-dimensional Laplace equation
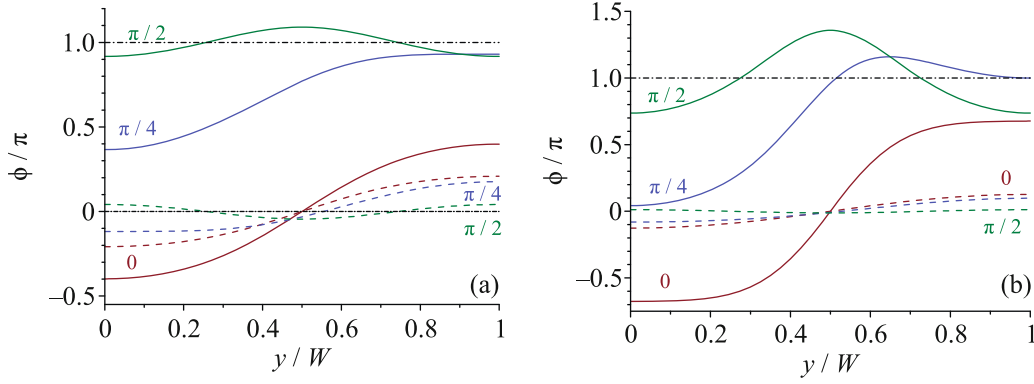
$$\Delta\psi(\mathbf{r}) = 0 \quad (10)$$

in an infinite strip $|x| < \infty$, $0 \leq y \leq W$ with the following boundary conditions at the edges $y = 0$ and $y = W$:

$$\partial_y\psi|_{y=0,W} = -\partial_y(\phi_+^\alpha + \phi_-^\alpha)|_{y=0,W}, \quad (11)$$

which can be written as [77]

$$\psi(\mathbf{r}) = \frac{\alpha_0 R^2}{4\pi}\int_{-\infty}^{+\infty}du[f_w(u)Q_w(\mathbf{r},u) - f_d(u)Q_d(\mathbf{r},u)],$$

$$Q_{d(w)}(\mathbf{r},u) = \ln\left[\cosh\left(\pi\frac{x-u}{W}\right) \mp \cos\left(\frac{\pi y}{W}\right)\right], \quad (12)$$

Fig. 2. (Color online) Phase distribution of the wavefunction $\phi((x_s, y)$ specified by Eqs., (8), (9), and (12) in two cross sections $x_s = $ (solid lines) 0 and (dashed lines) W of the electrode S_2 for three orientations $\chi = 0$, $\pi/4$, and $\pi/2$ of the exchange field of the ferromagnetic insulator disk and $x_d = $ (a) $0.5W$ and (b) $0.3W$. The calculations were performed with $\alpha_0 R^2/W = 1$, $R = 0.25W$, and $y_d = 0.5W$.

$$f_{d(w)}(u) = \frac{\cos\chi}{u_{d(w)+}^2} \mp \frac{2y_{d(w)}[(u - x_d)\sin\chi \pm y_{d(w)}\cos\chi]}{u_{d(w)+}^4}$$

$$+ \frac{\cos\chi}{u_{d(w)-}^2} \pm \frac{2y_{d(w)}[(u + x_d)\sin\chi \mp y_{d(w)}\cos\chi]}{u_{d(w)-}^4},$$

where $y_w = W - y_d$, $u_{d\pm}^2 = (u \mp x_d)^2 + y_d^2$, and $u_{w\pm}^2 = (u \mp x_d)^2 + y_w^2$.

Expressions (8), (9), and (12) determine the order parameter phase distribution $\phi(x,y)$ in the inhomogeneous state arising in a narrow SC strip with the planar Josephson junction at $x \geq 0$ under the exchange field of the FI disk and the Rashba spin–orbit coupling at the superconductor–ferromagnet interface. The phase $\phi(x,y)$ is determined up to an arbitrary value φ_0, which corresponds to the phase difference for the order parameters in the electrodes S_1 and S_2 far from the junction region and the FI disk, where the homogeneous SC state is established. Figure 2 shows the phase distributions $\phi(x,y)$ for two cross sections of the electrode S_2 at different orientations of the exchange field of the FI disk. It can be seen in Fig. 2 that the phase distribution $\phi(x_s, y)$ in the cross section $x_s = W$ on the right of the disk (dashed lines) becomes almost uniform even at $x_s - x_d \gtrsim R$. The nonuniform phase distribution $\phi(0, y)$ in the junction plane induced by the FI disk (solid lines) depends significantly on the orientation of the exchange field **h** and the position of the FI disk. As expected, the modulation amplitude of the phase $\phi(0, y)$ increases with a decrease in the distance $x_d - R$ between the disk and the junction.

Below, we consider the case where the FI disk is centered symmetrically with respect to the edges of the SC strip (i.e., $y_d = W/2$). Since the width W of the SC electrodes is an obvious spatial scale in the structure

under consideration, one can pass to dimensionless variables and express all distances in terms of W. In this case, $y_w = y_d$, $u_{w\pm} = u_{d\pm}$, and the expression for $\psi_0(y) = \psi(0,y)$ (12) can be simplified to the form

$$\psi_0(y) = \frac{\alpha_0 R^2}{4\pi W}$$

$$\times \left\{ \cos\chi \int_{-\infty}^{+\infty} du\, A(u)[Q_w(0, y, u) - Q_d(0, y, u)] \right.$$

$$\left. + \sin\chi \int_{-\infty}^{+\infty} du\, B(u)[Q_d(0, y, u) + Q_w(0, y, u)] \right\}, \quad (13)$$

where

$$A(u) = \frac{(u - x_d)^2 - y_d^2}{[(u - x_d)^2 + y_d^2]^2} + \frac{(u + x_d)^2 - y_d^2}{[(u + x_d)^2 + y_d^2]^2},$$

$$B(u) = \left[\frac{2y_d(u - x_d)}{[(u - x_d)^2 + y_d^2]^2} - \frac{2y_d(u + x_d)}{[(u + x_d)^2 + y_d^2]^2} \right].$$

In the limiting case of low transparency of the insulating barrier ($j_c \to 0$), the found distribution of the order parameter phase $\phi(x,y) + \varphi_0$ in the electrode S_2 determines the Josephson phase difference $\varphi(y) + \varphi_0 = \phi(0, y) + \varphi_0$ at the planar junction, where

$$\varphi(y) = \frac{\alpha_0 R^2}{W} \frac{x_d \sin\chi + (y - y_d)\cos\chi}{x_d^2 + (y - y_d)^2} + \psi_0(y). \quad (14)$$

The modulation amplitude of the Josephson phase difference (14) depends on the dimensionless parameter $\alpha_0 R^2/W$, which describes the total influence of spontaneous supercurrent (2) on the planar junction.
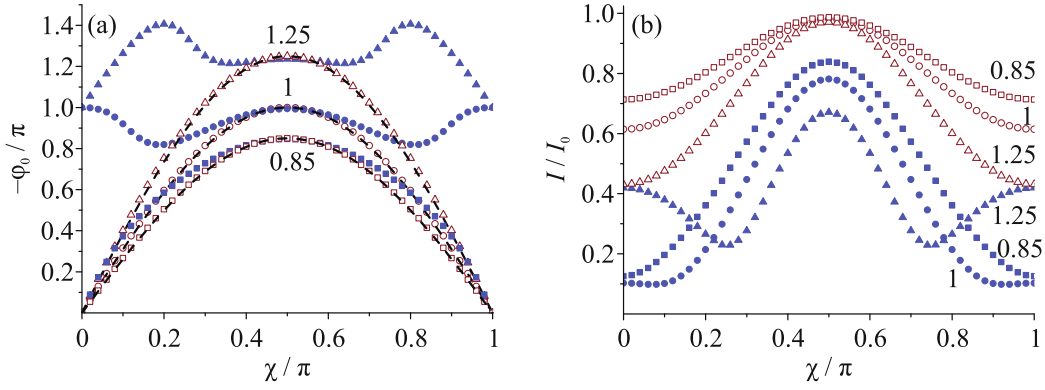
Fig. 3. (Color online) (a) Phase shift φ_0 and (b) critical current I_c versus the direction of the exchange field χ for three values $\alpha_0 R^2/W = 0.85$, 1, and 1.25 and two distances x_d = (closed symbols) $0.5W$ and (open symbols) $0.3W$ from the center of the ferromagnetic insulator disk to the junction. The calculations were performed with $R = 0.25W$ and $y_d = 0.5W$. The dashed lines in panel (a) plotted according to Eq. (16).

For the constant j_c value and sinusoidal dependence of the supercurrent density through the junction on the phase difference, the ground state of the Josephson junction in the hybrid structure under consideration corresponds to the minimum energy

$$E_J(\varphi_0) = \frac{\hbar I_0}{2e}\left[1 - \int_0^1 dy\cos\left[\varphi(y) + \varphi_0\right]\right], \quad (15)$$

where $I_0 = j_c dW$ is the maximum supercurrent in the planar junction, Eq. (14) for $\varphi(y)$ determines the modulation of the phase difference across the junction, and φ_0 is the difference of the order parameters phase between the electrode cross sections S_1 and S_2 far from the junction region and the FI disk, where the homogeneous (in space coordinates) SC state is established. The minimum energy (15) determines the phase shift $\varphi_0 = -\arctan\left(S_\varphi/C_\varphi\right)$ in the current–phase relation $I(\varphi) = I_c\sin(\varphi + \varphi_0)$, where $I_c = I_0\sqrt{S_\varphi^2 + C_\varphi^2}$ is the critical current of the φ_0 junction and

$$S_\varphi = \int_0^1 dy\sin\left(\varphi(y)\right), \quad C_\varphi = \int_0^1 dy\cos\left(\varphi(y)\right).$$

Figure 3 shows the dependences of the phase shift φ_0 and the critical current I_c on the orientation of the exchange field of the FI disk for several $\alpha_0 R^2/W$ values, which demonstrate that this superconductor–ferromagnet hybrid structure can be used to create an anomalous Josephson junction with the phase shift φ_0 smoothly varying over the wide range of $0-\pi$. The hybrid φ_0 junction consists of the planar Josephson junction and an external phase battery, which ensures smooth tuning of both the phase shift φ_0 and the critical current I_c of the structure as a whole. If the distance between the disk and the junction is not too small ($x_d > 2R$) and $\alpha_0 R^2/W \lesssim 1$, the modulation of the Josephson phase difference is weak ($|\varphi(y) + \varphi_0| \ll \pi$) and the critical current I_c decreases slightly in comparison with the maximum value I_0; hence, the phase shift φ_0 can be estimated as (see the supplementary materials)

$$\varphi_0 \approx -\int_0^1 dy\varphi(y) = -\frac{\pi\alpha_0 R^2}{W}\sin\chi. \quad (16)$$

This simple estimate for φ_0 is in good agreement with the calculated results (dashed lines in Fig. 3a). Note that the phase difference φ and the phase shift φ_0 are determined between the electrode cross sections, which are quite distant from the junction region and the FI disk, where the homogeneous SC state is restored; i.e., the hybrid Josephson structure includes the tunnel junction and the portion of the electrode S_2 where the spatial distribution of the transport current deviates from the uniform one. The spontaneous supercurrent generated by the FI disk and the spin–orbit coupling changes the kinetic inductivity of the electrode, forming an additional phase difference φ_0. A similar modification of the current–phase relation $I(\varphi)$ in superconductor–normal-metal–superconductor Josephson structures, which includes the inductance due to supercurrent redistribution in electrodes, was considered in [78, 79].

To summarize, the properties of the hybrid φ_0 junction consisting of a planar Josephson junction and an external phase battery formed by a ferromagnetic insulator disk on the surface of one of the superconducting junction electrodes in the presence of the Rashba spin–orbit coupling at the superconductor–ferromagnet interface have been studied. The main distinguishing feature of this device is the possibility of varying

the phase shift in the current−phase relation $I(\varphi) = I_c \sin(\varphi + \varphi_0)$ smoothly and over a wide range (from 0 to π) by changing the direction of the magnetization vector in the ferromagnetic insulator layer while the critical current I_c is retained almost constant.

SUPPLEMENTARY INFORMATION

The online version contains supplementary material available at https://doi.org/10.1134/S0021364024600411.

CONFLICT OF INTEREST

The author of this work declares that he has no conflicts of interest.

REFERENCES

1. K. V. Samokhin, Ann. Phys. **324**, 2385 (2009).
2. Yu. M. Shukrinov, Phys. Usp. **65**, 317 (2022).
3. M. Nadeem, M. S. Fuhrer, and X Wang, Nat. Rev. Phys. **5**, 558 (2023).
4. A. Buzdin and A. E. Koshelev, Phys. Rev. B **67**, 220504 (2003).
5. A. Buzdin, Phys. Rev. Lett. **101**, 107005 (2008).
6. K. K. Likharev, Rev. Mod. Phys. **51**, 101 (1979).
7. A. A. Golubov, M. Y. Kupriyanov, and E. Il'ichev, Rev. Mod. Phys. **76**, 411 (2004).
8. L. N. Bulaevskii, V. V. Kuzii, and A. A. Sobyanin, JETP Lett. **25**, 290 (1977).
9. A. I. Buzdin, L. N. Bulaevskii, and S. V. Panyukov, JETP Lett. **35**, 178 (1982).
10. A. I. Buzdin and M. Yu. Kupriyanov, JETP Lett. **53**, 321 (1991).
11. V. V. Ryazanov, V. Oboznov, A. Rusanov, A. Veretennikov, A. Golubov, and J. Aarts, Phys. Rev. Lett. **86**, 2427 (2001).
12. A. I. Buzdin, Rev. Mod. Phys. **77**, 935 (2005).
13. V. B. Geshkenbein and A. I. Larkin, JETP Lett. **43**, 395 (1986).
14. S. K. Yip, Phys. Rev. B **52**, 3087 (1995).
15. Y. Tanaka and S. Kashiwaya, Phys. Rev. B **56**, 892 (1997).
16. E. Goldobin, D. Koelle, R. Kleiner, and A. Buzdin, Phys. Rev. B **76**, 224523 (2007).
17. H. Sickinger, A. Lipman, M. Weides, R. G. Mints, H. Kohlstedt, D. Koelle, R. Kleiner, and E. Goldobin, Phys. Rev. Lett. **109**, 107002 (2012).
18. I. I. Soloviev, N. V. Klenov, S. V. Bakurskiy, V. V. Bol'ginov, V. V. Ryazanov, M. Yu. Kupriyanov, and A. A. Golubov, Appl. Phys. Lett. **105**, 242601 (2014).
19. F. Konschelle, I. V. Tokatly, and F. S. Bergeret, Phys. Rev. B **92**, 125445 (2015).
20. M. A. Silaev, I. V. Tokatly, and F. S. Bergeret, Phys. Rev. B **95**, 184508 (2017).
21. D. B. Szombati, S. Nadj-Perge, D. Car, S. R. Plissard, E. P. A. M. Bakkers, and L. P. Kouwenhoven, Nat. Phys. **12**, 586 (2016).
22. E. Strambini, A. Iorio, O. Durante, R. Citro, C. Sanz-Fernandez, C. Guarcello, I. V. Tokatly, A. Braggio, M. Rocci, N. Ligato, V. Zannier, L. Sorba, F. S. Bergeret, and F. A. Giazotto, Nat. Nanotechnol. **15**, 656 (2020).
23. A. Assouline, C. Feuillet-Palma, N. Bergeal, T. Zhang, A. Mottaghizadeh, A. Zimmers, E. Lhuillier, M. Eddrie, P. Atkinson, M. Aprili, and H. Aubin, Nat. Commun. **10**, 126 (2019).
24. W. Mayer, M. C. Dartiailh, J. Yuan, K. S. Wickramasinghe, E. Rossi, and J. Shabani, Nat. Commun. **11**, 212 (2020).
25. S. Pal and C. Benjamin, Eur. Phys. Lett. **126**, 57002 (2019).
26. A. K. Feofanov, V. A. Oboznov, V. V. Bol'ginov, J. Lisenfeld, S. Poletto, V. V. Ryazanov, A. N. Rossolenko, M. Khabipov, D. Balashov, A. B. Zorin, P. N. Dmitriev, V. P. Koshelets, and A. V. Ustinov, Nat. Phys. **6**, 593 (2010).
27. E. Goldobin, H. Sickinger, M. Weides, N. Ruppelt, H. Kohlstedt, R. Kleiner, and D. Koelle, Appl. Phys. Lett. **102**, 242602 (2013).
28. I. I. Soloviev, N. V. Klenov, S. V. Bakurskiy, M. Y. Kupriyanov, A. L. Gudkov, and A. S. Sidorenko, Beilstein J. Nanotechnol. **8**, 2689 (2017).
29. R. Wakatsuki, Y. Saito, S. Hoshino, Y. M. Itahashi, T. Ideue, M. Ezawa, Y. Iwasa, and N. Nagaosa, Sci. Adv. **3**, e1602390 (2017).
30. A. Daido, Phys. Rev. Lett. **128**, 037001 (2022).
31. J. J. He, Y. Tanaka, and N. Nagaosa, New J. Phys. **24**, 053014 (2022).
32. T. Karabassov, I. V. Bobkova, A. A. Golubov, and A. S. Vasenko, Phys. Rev. B **106**, 224509 (2022).

33. A. V. Putilov, S. V. Mironov, and A. I. Buzdin, Phys. Rev. B **109**, 014510 (2024).

34. C. Baumgartner, L. Fuchs, A. Costa, S. Reinhardt, S. Gronin, G. C. Gardner, T. Lindemann, M. J. Manfra, P. E. Faria J., D. Kochan, J. Fabian, N. Paradiso, and C. Strunk, Nat. Nanotechnol. **17**, 39 (2022).

35. Ya. V. Fominov and D. S. Mikhailov, Phys. Rev. B **106**, 134514 (2022).

36. M. Alidoust and J. Linder, Phys. Rev. B **87**, 060503 (2013).

37. I. I. Soloviev, N. V. Klenov, S. V. Bakursky, M. Yu. Kupriyanov, and A. A. Golubov, JETP Lett. **101**, 240 (2015).

38. A. V. Ustinov, Appl. Phys. Lett. **80**, 3153 (2002).

39. E. Goldobin, A. Sterck, T. Gaber, D. Koelle, and R. Kleiner, Phys. Rev. Lett. **92**, 057005 (2004).

40. E. Goldobin, S. Mironov, A. Buzdin, R. G. Mints, D. Koelle, and R. Kleiner, Phys. Rev. B **93**, 134514 (2016).

41. S. L. Miller, K. R. Biaga, J. R. Clem, and D. K. Finnemore, Phys. Rev. B **31**, 2684 (1985).

42. A. A. Golubov and M. Yu. Kupriyanov, Sov. Phys. JETP **65**, 849 (1987).

43. M. V. Fistul', JETP Lett. **52**, 192 (1990).

44. T. Golod, A. Rydh, and V. M. Krasnov, Phys. Rev. Lett. **104**, 227003 (2010).

45. T. Golod, R. A. Hovhannisyan, O. M. Kapran, V. V. Dremov, V. S. Stolyarov, and V. M. Krasnov, Nano Lett. **21**, 5240 (1921).

46. A. A. Fraerman, S. A. Gusev, Y. N. Nozdrin, A. V. Samokhvalov, S. N. Vdovichev, L. Fritzsch, E. Il'ichev, and R. Stolz, Phys. Rev. B **73**, 100503 (2006).

47. A. V. Samokhvalov, J. Exp. Theor. Phys. **104**, 451 (2007).

48. A. V. Samokhvalov, S. N. Vdovichev, B. A. Gribkov, S. A. Gusev, A. Yu. Klimov, Yu. N. Nozdrin, V. V. Rogov, A. A. Fraerman, S. V. Egorov, V. V. Bol'ginov, A. B. Shkarin, and V. S. Stolyarov, JETP Lett. **95**, 104 (2012).

49. J. Chang, V. L. Mironov, B. A. Gribkov, A. A. Fraerman, S. A. Gusev, and S. N. Vdovichev, J. Appl. Phys. **100**, 104304 (2006).

50. A. V. Samokhvalov, Phys. Rev. B **80**, 134513 (2009).

51. P. M. Tedrow, J. E. Tkaczyk, and A. Kumar, Phys. Rev. Lett. **56**, 1746 (1986).

52. T. Tokuyasu, J. A. Sauls, and D. Rainer, Phys. Rev. B **38**, 8823 (1988).

53. A. Hijano, S. Ilić, M. Rouco, C. Gonzalez-Orellana, M. Ilyn, C. Rogero, P. Virtanen, T. T. Heikkila, S. Khorshidian, M. Spies, N. Ligato, F. Giazotto, E. Strambini, and F. S. Bergeret, Phys. Rev. Res. **3**, 023131 (2021).

54. A. A. Kopasov and A. S. Mel'nikov, Phys. Rev. B **105**, 214508 (2022).

55. I. V. Bobkova, A. M. Bobkov, and M. A. Silaev, J. Phys.: Condens. Matter **34**, 353001 (2022).

56. T. T. Heikkila, M. Silaev, P. Virtanen, and F. S. Bergeret, Prog. Surf. Sci. **94**, 100540 (2019).

57. L. P. Gor'kov and E. I. Rashba, Phys. Rev. Lett. **87**, 037004 (2001).

58. V. M. Edelstein, Phys. Rev. B **67**, 020505 (2003).

59. E. I. Rashba, Sov. Phys. Solid State **2**, 1109 (1960).

60. V. M. M. Edel'shtein, Sov. Phys. JETP **68**, 1244 (1989).

61. V. M. Edelstein, Phys. Rev. Lett. **75**, 2004 (1995).

62. S. S. Pershoguba, K. Björnson, A. M. Black-Schaffer, and A. V. Balatsky, Phys. Rev. Lett. **115**, 116602 (2015).

63. A. G. Mal'shukov Phys. Rev. B **93**, 054511 (2016).

64. J. Baumard, J. Cayssol, F. S. Bergeret, and A. Buzdin, Phys. Rev. B **99**, 014511 (2019).

65. A. V. Samokhvalov, J. Exp. Theor. Phys. **135**, 897 (2022).

66. J. W. A. Robinson, A. V. Samokhvalov, and A. I. Buzdin, Phys. Rev. B **99**, 180501(R) (2019).

67. A. V. Samokhvalov, A. A. Kopasov, A. G. Kutlin, S. V. Mironov, A. I. Buzdin, and A. S. Mel'nikov, JETP Lett. **113**, 34 (2021).

68. J. Pearl, Appl. Phys. Lett. **5**, 65 (1964).

69. L. A. B. Olde Olthof, X. Montiel, J. W. A. Robinson, and A. I. Buzdin, Phys. Rev. B **100**, 220505(R) (2019).

70. A. G. Mal'shukov, Phys. Rev. B **101**, 134514 (2020).

71. A. G. Mal'shukov, Phys. Rev. B **102**, 144503 (2020).

72. V. P. Mineev, K. V. Samokhin, Sov. Phys. JETP **78**, 401 (1994).

73. D. F. Agterberg, Phys. C (Amsterdam, Neth.) **387**, 13 (2003).

74. Yu. M. Ivanchenko and S. K. Soboleva, Sov. Phys. Solid State **32**, 1181 (1990).

75. V. G. Kogan, V. V. Dobrovitski, J. R. Clem, Y. Mawatari, and R. G. Mints, Phys. Rev. B **63**, 144501 (2001).

76. M. Moshe, V. G. Kogan, and R. G. Mints, Phys. Rev. B **78**, 020510(R) (2008).

77. A. D. Polyanin, *Handbook on Mathematics for Engineers and Scientists* (Fizmatlit, Moscow, 2001; CRC, Chapman and Hall, Boca Raton, FL, 2006).

78. A. A. Zubkov, M. Yu. Kupriyanov, and V. K. Semenov, Sov. J. Low Temp. Phys. **7**, 661 (1981).

79. V. Ruzhickiy, S. Bakurskiy, M. Kupriyanov, N. Klenov, I. Soloviev, V. Stolyarov, and A. Golubov, Nanomaterials **13**, 1873 (2023).

Translated by A. Sin'kov